General Disclaimer

One or more of the Following Statements may affect this Document

- This document has been reproduced from the best copy furnished by the organizational source. It is being released in the interest of making available as much information as possible.

- This document may contain data, which exceeds the sheet parameters. It was furnished in this condition by the organizational source and is the best copy available.

- This document may contain tone-on-tone or color graphs, charts and/or pictures, which have been reproduced in black and white.

- This document is paginated as submitted by the original source.

- Portions of this document are not fully legible due to the historical nature of some of the material. However, it is the best reproduction available from the original submission.

Closing the Design Loop on HiMAT (Highly Maneuverable Aircraft Technology)

Terrill W. Putnam and M. R. Robinson

December 1984

Closing the Design Loop on HiMAT (Highly Maneuverable Aircraft Technology)

Terrill W. Putnam
NASA Ames Research Center, Dryden Flight Research Facility, Edwards, California
M. R. Robinson
Rockwell International, Los Angeles, California

1984

CLOSING THE DESIGN LOOP ON HIMAT
(HIGHLY MANEUVERABLE AIRCRAFT TECHNOLOGY)

Terrill W. Putnam   and   M. R. Robinson
NASA Ames - Dryden   Rockwell International

ABSTRACT

The design methodology used in the HiMAT program will be discussed along with the wind tunnel development activities. Selected results from the flight test program will be presented and the strengths and weaknesses of testing advanced technology vehicles using the RPV concept will be discussed. The role of simulation in the development of digital flight control systems and in RPV's in particular will be emphasized.

INTRODUCTION

Many advanced aircraft technology concepts developed in the early 1970's promised to enhance significantly the transonic maneuverability of fighter aircraft. The maximum potential of these benefits were predicted to be realized only if the technologies were synergistically blended and integrated. NASA and the Air Force therefore initiated the highly maneuverable aircraft technology (HiMAT) program to demonstrate the benefits of integrating as many advanced technologies as practical into one vehicle. In addition to demonstrating the advanced technology benefits in flight, the program provided the opportunity to validate the design processes employed. To ensure that the design team was suitably challenged, NASA established that the vehicle have the ability to perform a sustained 8g turn at Mach 0.9, at an altitude of 30,000 feet, with a mission radius of 300 nautical miles. In August 1975, Rockwell International was awarded a contract to design a full-scale fighter airplane to meet this maneuvering goal, and to design and build two subscale aircraft capable of demonstrating the integrated benefits of the advanced concepts incorporated in the full-scale design. Two 0.44-scale aircraft were delivered to the NASA Dryden Flight Research Center in March and June 1978.

One of the major research objectives of the HiMAT program was the use of computational tools in the aerodynamic and structural design efforts to minimize the use of the more expensive wind tunnel and laboratory tests. Based on previous experience, it was recognized that both manned and unmanned simulations would be used extensively in the design and qualification of the flight control system.

The major flight test program objective was to demonstrate the performance capability of the HiMAT vehicles and to provide high-quality flight test data for correlation and comparison with design data.

VEHICLE DESCRIPTION

The HiMAT remotely piloted research vehicle (RPRV) is a 0.44-scale model of a 17,000-pound fighter airplane (Figure 1). The 3,055-pound (maneuver design weight) RPRV has a wing span of 15.6 feet and a length of 23.5 feet including the flight test nose boom (Figure 2). It is powered by a GE J85-21 afterburning turbojet engine.

The advanced technologies incorporated in the full scale HiMAT fighter design are also shown in Figure 2. The items followed by an asterisk (*) were only partially implemented on the HiMAT RPRV vehicles; the others were fully integrated.
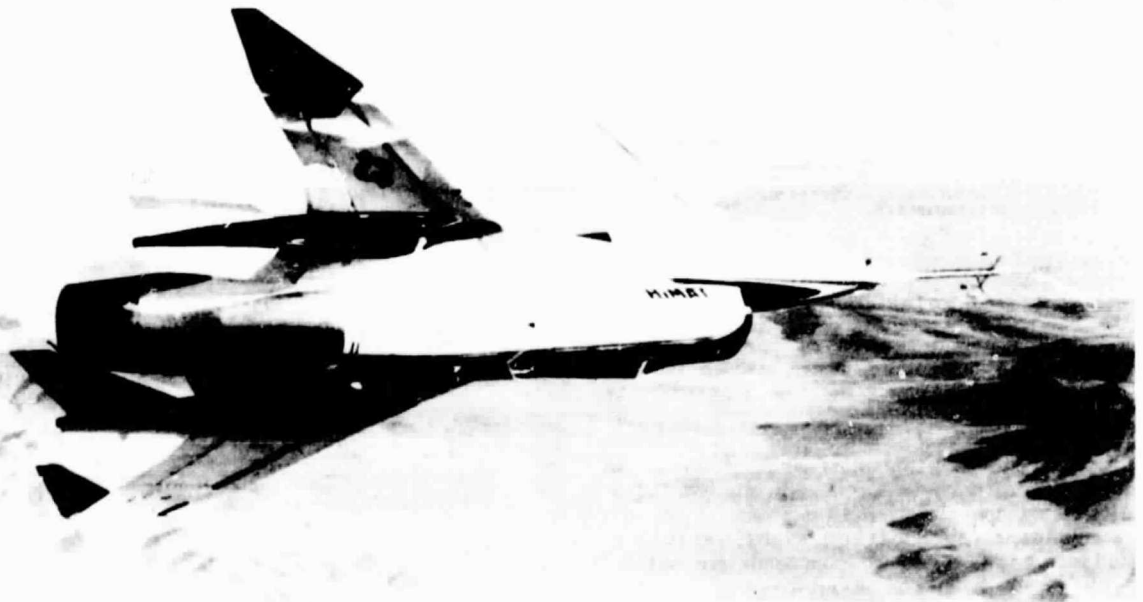

Figure 1. HiMAT Remotely Piloted Research Vehicle

Technologies

- Close-coupled canard
- Digital FBW control system
- Relaxed static stability
- Composite structure*
- Aeroelastic tailoring
- Variable camber*
- Direct lift and side forces*
- Supercritical airfoil
- Wingtip fins
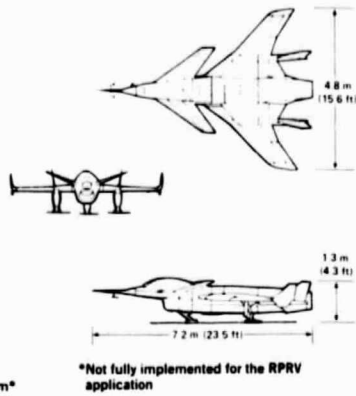- Integrated propulsion control system*

*Not fully implemented for the RPRV application

4.8 m (15.6 ft)

1.3 m (4.3 ft)

7.2 m (23.5 ft)

Figure 2. HiMAT Technologies and Design

Figure 4. HiMAT RPRV Control System

OPERATIONAL CONCEPT

The HiMAT vehicles were designed to be air-launched from a specially modified B-52 aircraft. The operational concept for the HiMAT vehicle (Figure 3) is similar to that for previous RPRV's flown at NASA Dryden. The 3,370-lb vehicle is launched at 45,000 feet, and carries 660 pounds of fuel. The vehicle is controlled by a NASA research test pilot in a ground-based RPRV facility cockpit. Flight test activity is monitored on the ground. Vehicle response parameters for use in the control laws are obtained by use of a telemetry downlink. Flight control laws for both primary and backup operation are implemented through two groundbased and two airborne digital computers. The vehicle is equipped with landing skids and forward-looking television for horizontal recovery on the surface of the Edwards Dry Lake.
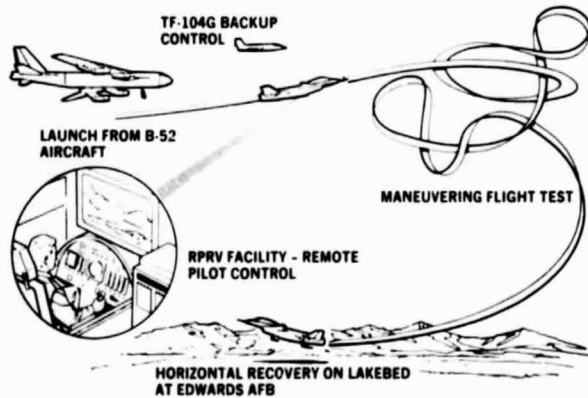
Figure 3. HiMAT Operational Concept

In the primary mode of operation (Figure 4), aircraft sensor data are transmitted to the ground by the telemetry downlink. The downlinked data are used both to drive the ground cockpit and as input to the ground-based control law computer. The control law computer combines the pilot input commands with the downlinked aircraft sensor data in the execution of the HiMAT control laws, then formats a servoactuator command for each of the eight vehicle control surfaces. These surface commands are output to the uplink encoder and then transmitted to the aircraft.[1]
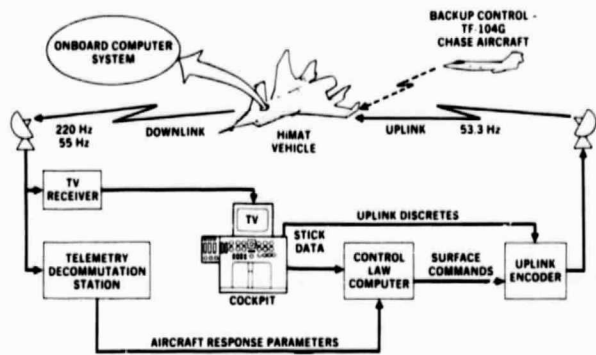
AERODYNAMIC AND STRUCTURAL DESIGN

Closing the design loop on HiMAT was an iterative process which started shortly after the 1975 contract award and continued until correlations between design, ground test, and flight test were completed in 1984. Most of the actual learning was accrued during the design and manufacturing phases; final verification and, therefore, credibility of that learning was provided by the flight test program. This process (Figure 5), implies the tremendous benefit of having experimental prototype programs. It is often argued that technologies can be sufficiently developed without the expense of building a new flight vehicle. There is evidence to support this premise when technologies are considered individually, but primary management concerns in developing new systems for production are:

1. The compromises necessary to integrate several new technologies into a system with real constraints must allow a significant level of benefit of the technology to be realized.

2. The "unknown unknowns" that are often discovered when attempting to include numerous new technologies into a new system. Late discovery of these unpredictable problems may significantly impact cost and/or schedule performance.

HiMAT provided the basis to minimize these concerns for a suite of aerodynamic, control, and structural technologies now being employed in both derivatives of current fighters and in new designs.
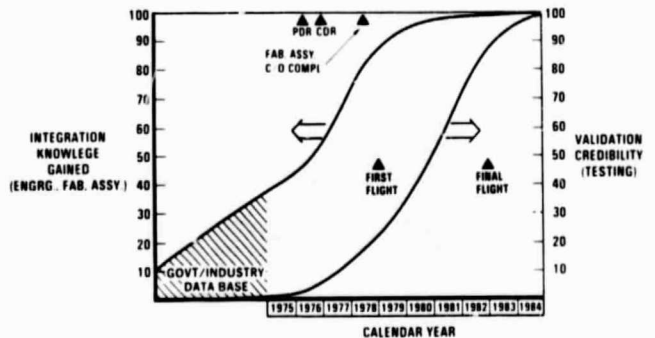
Figure 5. HiMAT Learning and Validation Experience

Design Integration

The HiMAT aerodynamic development was driven by several unique configurational aspects.[2] In turn, the configuration was driven by several goals and constraints:

1. Most importantly, the need to integrate, to the highest fidelity possible, the 10 technologies shown in Figure 2

2. The configuration had to be representative of a realistic (future) air-to-air fighter

3. The additional constraints of scaling effects and RPRV requirement

4. The transonic sustained maneuver requirement of 8g's coupled with efficient 1g performance

The approach taken was first to design a full-scale fighter which included the desired technology integration, and to then develop the RPRV with minimum compromise to that full-size configuration.

In sizing the RPRV, it was desired to match the thrust-to-weight ratio (T/W) and the wing loading (W/S) of the full-scale fighter at combat conditions (mach 0.9, 30,000 foot altitude) so that equivalent maneuvering performance could be demonstrated. Within the constraints imposed by the availability of off-the-shelf J85-21 engines, the best match was found to be the 0.44 scale factor. This resulted in an RPRV launch gross weight of 3,370 pounds. Planform differences from the baseline fighter to the RPRV which resulted from the design process (discussed later) also dictated that the transonic maneuver point altitude for the RPRV be lowered to 25,000 feet. The comparison of fighter and RPRV characteristics resulting from this scaling is shown in Figure 6.
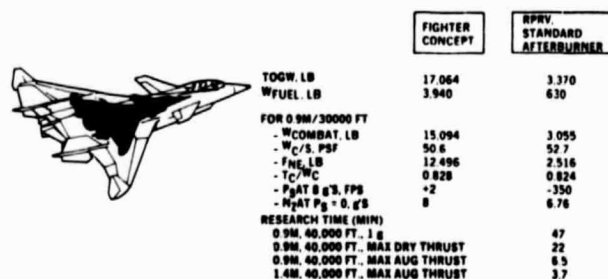
	FIGHTER CONCEPT	RPRV STANDARD AFTERBURNER
TOGW, LB	17,064	3,370
W_{FUEL}, LB	3,940	630
FOR 0.9M/30000 FT		
- W_{COMBAT}, LB	15,094	3,055
- W_C/S, PSF	50.6	52.7
- F_{NE}, LB	12,496	2,516
- T_C/W_C	0.828	0.824
- P_S AT 8 g'S, FPS	+2	-350
- N_T AT P_S = 0, g'S	8	6.76
RESEARCH TIME (MIN)		
0.9M, 40,000 FT., 1 g		47
0.9M, 40,000 FT., MAX DRY THRUST		22
0.9M, 40,000 FT., MAX AUG THRUST		6.5
1.4M, 40,000 FT., MAX AUG THRUST		3.7

Figure 6. Comparison of Fighter to RPRV

Perhaps the largest aerodynamic design challenge was to attain high lift-to-drag efficiency at 1g cruise, 8g maneuver, and throughout the intermediate region with a minimum of mechanical variable camber/twist devices. This challenge drove the implementation requirements for two of the key technologies, aeroelastic tailoring of wing and canard, and relaxed static longitudinal stability. Controlled supercritical flow was generally sought through the use of variable camber and elastic twist in conjunction with a longitudinal unstable balance which permitted wing trailing edge down deflections (favorable cambering) for trim. This was accomplished by controlling the wing and canard aeroelastic characteristics through structural tailoring in such a manner that deformation

due to application of lifting loads would result in a desired variation in twist from the root out to the tip, and an efficient spanwise load distribution. The required twist distribution for the desired load distribution is shown in figure 7. Not all of the twist was able to be provided by aeroelastic tailoring: a portion of it is built into the jig-shape, and the additional increment is provided by the mechanical leading edge variable camber feature.
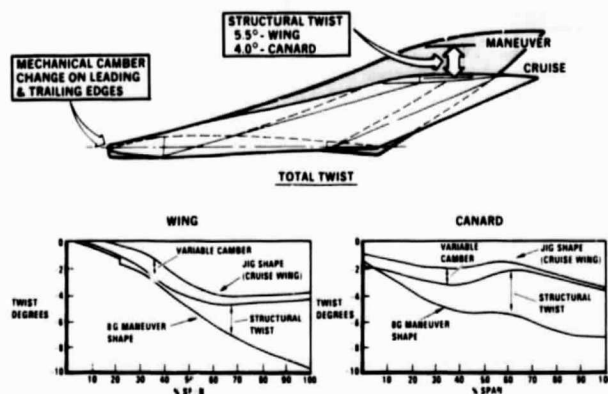

Figure 7. Aeroelastic Tailoring

Overall system aerodynamic performance is measured by trimmed lift-drag ratio. Comparison of the HiMAT with existing fighters at the design mach number is shown in Figure 8. One hundred percent improvement is realized in trim lift-to-drag ratio at a $C_L = 1.0$, and very substantial increases over a wide range of lift.

Design Methods Development

The broad-spectrum high lift-to-drag ratio requirement also severely challenged the development of lifting surface design methodology. The goal was to maintain attached flow from cruise conditions to the very high lift and angle of attack maneuver conditions. At lifts where attached flow cannot be maintained, controlled separated (vortex lift) flow is desired. This philosophy prevails even with current emphasis on efficient combined supersonic and transonic operation.

The methodology employed to implement this philosophy is two fold:

1. Linear theory to perform full configuration constrained span load optimization and define aeroelastic twist goals;

2. Nonlinear transonic relaxation theory (Bailey-Ballhaus and Bauer codes) to develop controlled (but shocked) supercritical flow to achieve separation minimization.

The numerical analysis was combined with scale-model force and pressure tests in a high-density wind tunnel in an iterative manner of design, test, redesign, and retest cycles. The HiMAT was the first three-dimensional application of transonic computational theory to a real aircraft. The development process was accomplished with four wind tunnel test entries encompassing 525 test hours. The impact of computational methodology is clear from the successful
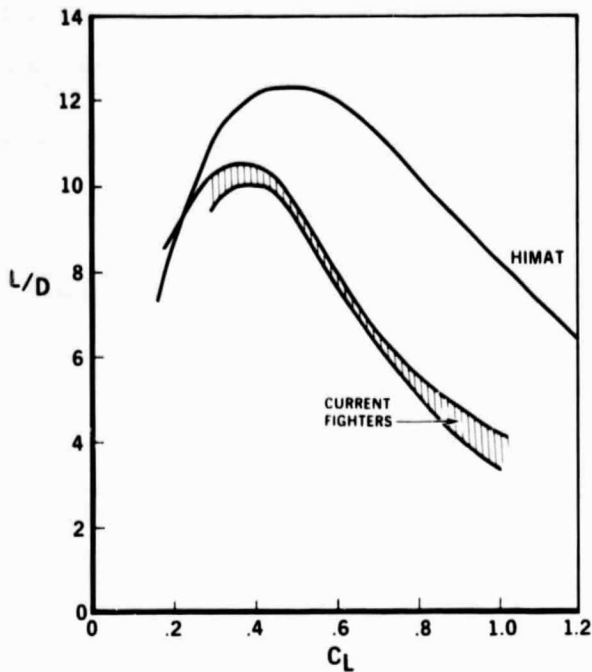
Figure 8. Transonic Lift-Drag Ratio Comparison at Mach 0.9

Structural Challenges

The HiMAT structural design philosophy was driven by three major factors:[3]

1. Aeroelastic tailoring to provide the aerodynamic required twist and camber distributions

2. Maximum use of advanced materials, both metallic and nonmetallic

3. Modular design so that components of the airplane could be replaced with alternate designs for research purposes

The modular breakdown of the vehicle is illustrated in Figure 9. The major interchangeable components include the propulsion module (aft fuselage), outer wing panels, canards, winglets, wing and canard leading edges, and forward portion of the inlet. The propulsion module break line was designed to accommodate a non-axisymmetric exhaust nozzle. The wings outboard of the tail booms can be removed and replaced with wings of other aerodynamic and/or structural concepts. The interchangeable leading edges permit testing of wing and canard camber variations. Funding considerations prevented utilization of these modularity features beyond the design stage.

results and relatively modest wind tunnel test effort required to achieve them. The HiMAT wing development effort also conclusively established the importance of a balanced approach between theory and experiment. Measurements directly led to theoretical code extensions to reconcile test results. Further improvement of the HiMAT maneuver performance relative to shock weakening is certainly possible today using full potential and Euler computational methodology.

Design Lessons

Early wind tunnel tests of the HiMAT RPRV model, based on the fighter configuration, indicated that the induced drag goals were not being met, and extreme nonlinearities existed in the pitching moment characteristics at high angles of attack. These test results led to the incorporation of several modifications to the RPRV configuration.

Wing and canard changes were made to obtain the necessary span loading required to achieve the induced drag goals within practical spanwise twist variation limitations. The chord of the outboard wing was lengthened to reduce section lift coefficient, and loading was transferred from the inboard wing to the canard. The canard trailing edge was moved forward to eliminate unfavorable interference where the canard and wing overlapped.

It was desired to increase the vertical separation between the wing and canard to improve the wing load distribution, but the shallow fuselage precluded raising the canard. Increased dihedral of the canard was found to be a satisfactory alternative. Due to the increased dihedral, lateral-directional characteristics at low angles of attack were degraded. This situation was corrected by the addition of lower surface winglets and increased vertical tail volume.
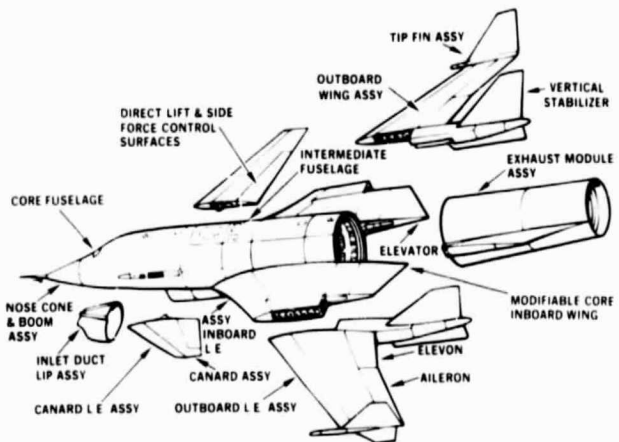

Figure 9. Modularity Features

The HiMAT design made use of several advanced materials and composite structure applications. This contributed to program objectives of demonstrating weight and cost reduction technologies. Figure 10 shows the general HiMAT structural concept and the breakdown of materials. There are advanced materials and construction techniques in both primary and secondary structures.

On the basis of extensive trade studies, actual design, and fabrication experience with HiMAT, it has been established that graphite/epoxy is the prime candidate material for primary and secondary lifting surface structures. Other recent programs verify this finding. Control and lifting surfaces are designed, at least in part, by torsional stiffness requirements to resist wrap-up and to attain the torsional/bending stiffness requirements for flutter. The significant weight savings attainable by application of graphite/epoxy for stiffness-governed designs have been

4

well documented, and overall savings of 25 to 40 percent are obtained from these applications.
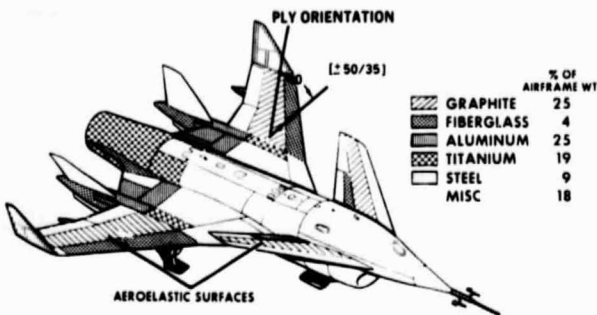

Figure 10. Advanced Structural Technology

The design requirement initially specified for aeroelastic tailoring of the wing (Figure 6) was 9.5 degrees of twist (washout) at the wing tip at the 8g loading condition. It was originally planned that 2 degrees twist would be built into the jig shape of the airplane, and the remaining 7.5 degrees would be achieved through aeroelastic deformation of the wing structure. However, from the results of comprehensive design iterations of the effects of composite material ply orientation, various composite materials, and alternate structural arrangements, it was concluded that 5.5 degree twist at the wing tip was the maximum that could be achieved with aerodynamics. A major constraint to the aeroelastic tailoring process was the modular design concept

wherein the outboard wing panel was made an interchangeable component. The resulting structural arrangement dictated that nearly all of the desired aeroelastic deformation be provided by the outboard wing panel.

Structural Methods Development

Similar to the aerodynamic design experience, the development of structural design tools, especially those for application to aeroelastic composite lifting surfaces, was challenged and focused within the HiMAT program.[3] This is the first known attempt to utilize the TSO composite design optimatization computer program. Though these first attempts were not totally successful, the lessons learned led to numerous improvements in the program. Because of this experience and continued work, TSO is a valuable and credible tool for rapid optimization at the preliminary design level.

FABRICATION

The HiMAT served as a flight test system to verify advanced manufacturing technologies and developments. As shown in Figure 11, HiMAT's size presented the formidable challenge of packaging a full-size J85-21 engine as well as 13 onboard subsystems within a scaled down fighter.

Some of the more signicant fabrication issues encountered were:

1. To minimize the assembly tool cost associated with only two vehicles with no duplicate tooling, subassembly tools were utilized to become mate position tools. Further, by accelerating the
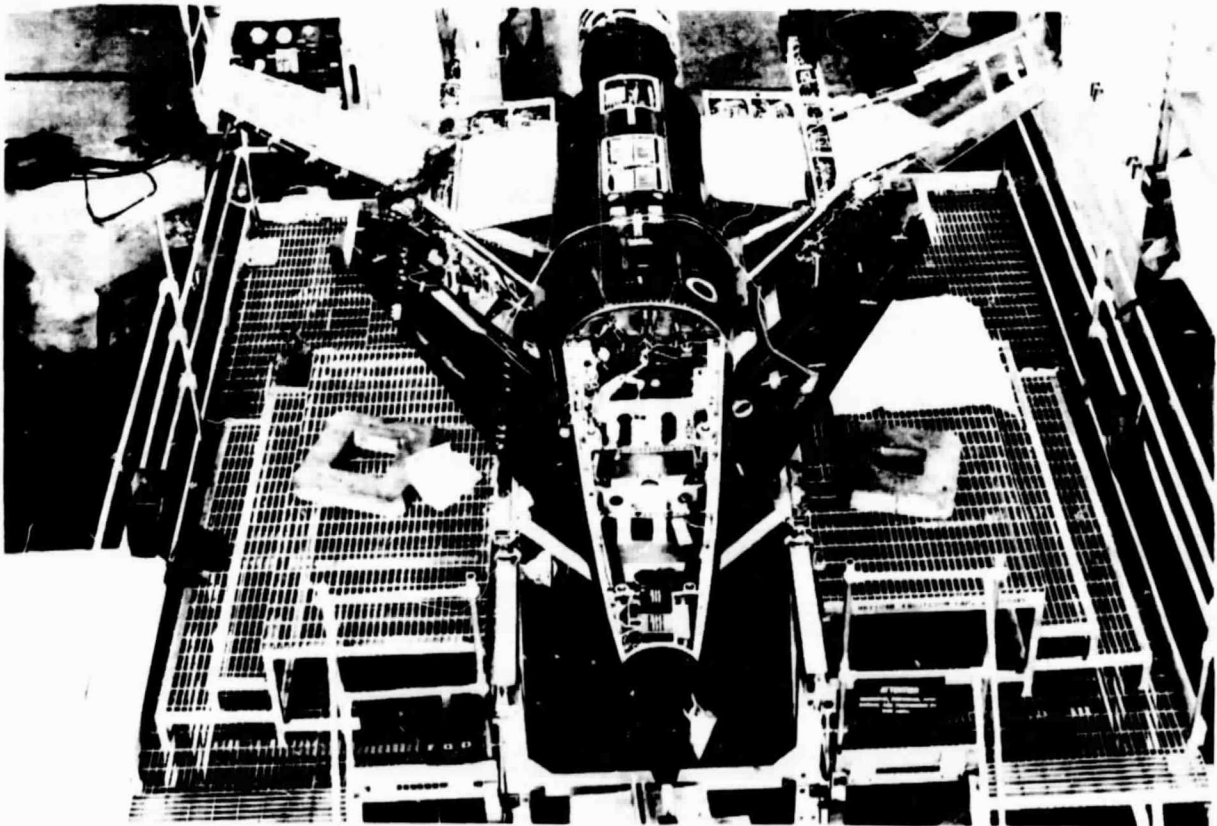

Figure 11. HiMAT in Fabrication

fabrication of the ground equipment required for the flight test program, they could be used for final assembly and checkout.

2. As a result of a lack of a design data base throughout the industry for nonstandard skin ply orientations, a quick response materials and processes test program was carried out to establish a design criteria data base.

3. The high amount of composite skins with outer moldline (OML) critical tolerance required vehicle tooling to be OML controlled. This led to development of a low-cost master model fabrication method.

In the fabrication of secondary-structure components for HiMAT (canard flaps, wing leading edges, engine inlet duct, tail body fairings, ailerons, and elevons), it was demonstrated that efficiently designed composite secondary structures result in piece-part count reductions and fewer manufacturing operations. These discoveries when applied in production, are expected to lead to cost savings of 10 to 25 percent.

Development of other new lower-cost tool and part fabrication methods include hydratool layup dies, ceramic layup dies and bond jigs, batch forming of titanium parts, disposable mandrel layup dies, and development of low-cost nondestructive testing methods using a harmonic bond tester. The fabrication techniques developed enabled the HiMAT program to meet the technology challenge.

Many lessons were learned that have had impact on composite structure design and fabrication. One of the most pertinent is that while unbalanced, non-standard ply orientations (unequal numbers of plies at other than +45o and -45o) are feasible (Figure 10), the complexity of tooling and manufacturing them without warp makes assembly difficult. Thus, a rigorous cost/schedule/ aerodynamic requirement tradeoff should be conducted early to assist in selecting the appropriate design.

SIMULATION DESCRIPTION

Extensive simulations of the HiMAT flight vehicles and their associated ground-based control systems were used in the development and flight test of the vehicles.(4) The real-time manned simulations were primarily used for engineering purposes and secondarily used for pilot and procedural training. Figure 12 is a block diagram of the main elements of all the simulations. The uplink and downlink systems had to be accurately modeled to account for any time delays introduced through their use. In all, there were four different real-time simulations used at NASA with their differences characterized by intended use and the use of flight hardware and software in the simulation.
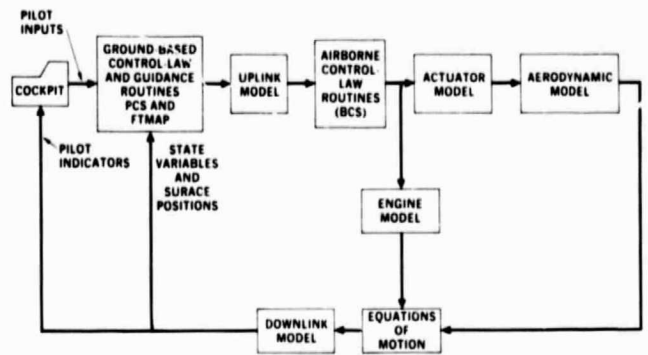

Figure 12. HiMAT Simulation System

The basic simulation was used for the design and analysis of both the primary control system (PCS) and the backup control system (BCS). There was no flight hardware used in this simulation; every element was modeled in the digital simulation computer which was connected to and controlled through the simulation cockpit (Figure 13).

The verification simulation was used to validate the PCS flight software in the ground-based control computers. The ground-based control law computers, classified as part of the flight control system, were used with the simulation cockpit. The remainder of the elements were modeled in software and resident in the simulation computers.
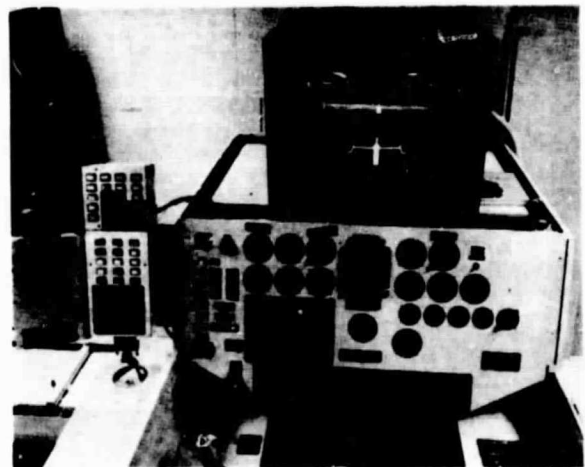

Figure 13. HiMAT Simulation Cockpit

The hot bench simulation was used to conduct system-wide verification and validation including redundancy management. It was also used for pilot training with and without failures induced in the system. Flight test engineers also made extensive use of this simulation for flight planning. The airborne and ground-based control law computers were interfaced with the simulation computer where the remainder of the elements were modeled.

The iron bird simulation was the fourth and most complicated simulation because it used the HiMAT vehicle itself (Figure 14). This simulation was used to monitor the operation and condition of the vehicle systems, validate all flight systems except the engine, conduct a full mission simulation and to train the pilot and flight test engineer. Flight hardware was extensively used including the remotely piloted research vehicle cockpit.

A summary of the advantages and disadvantages of each of the real-time simulations is given in Table I. All of the simulations were written in FORTRAN code; the code was therefore transportable between the various simulations. The hardware interfaces were complex and the timing was critical for these simulations to represent the vehicle and its control system accurately.

FLIGHT PROGRAM

The flight program was conceptually divided into two phases. The first phase was for envelope expansion and demonstration of the maneuver and design goals. The second was to acquire the flight data necessary for correlation and comparison with predictions. During the preparation for the first flight, however, it was decided that the first phase should be further subdivided with the vehicles to be initially flown statically stable and subsequently at relaxed static stability.

Table I. Real-Time Simulation Configuration Summary

CONFIGURATION	ADVANTAGES	DISADVANTAGES
Basic	• Best design evaluation tool • Least complicated system to use	• Computer time requirements are borderline for real-time operation
Verification	• Best primary control evaluation tool • Minimum system complexity using ground-based flight computers	• No backup control operation
Hot bench	• Best backup control evaluation tool • Optimum model of flight configuration with no vehicle impact	• Not good design tool • Complex system
Iron bird	• Maximum use of actual flight hardware • Best flight system validation configuration	• Complex system • Requires much dedicated hardware and personnel

The flight test program is summarized in Figure 15 with the mach/altitude envelope achieved over the course of the program. Ten captive flights were flown with both HiMAT vehicles attached to the B-52 airplane for the entire flight. Twenty-six free flights were flown with both vehicles over the 3-1/2 year flight test program. It should be noted that one
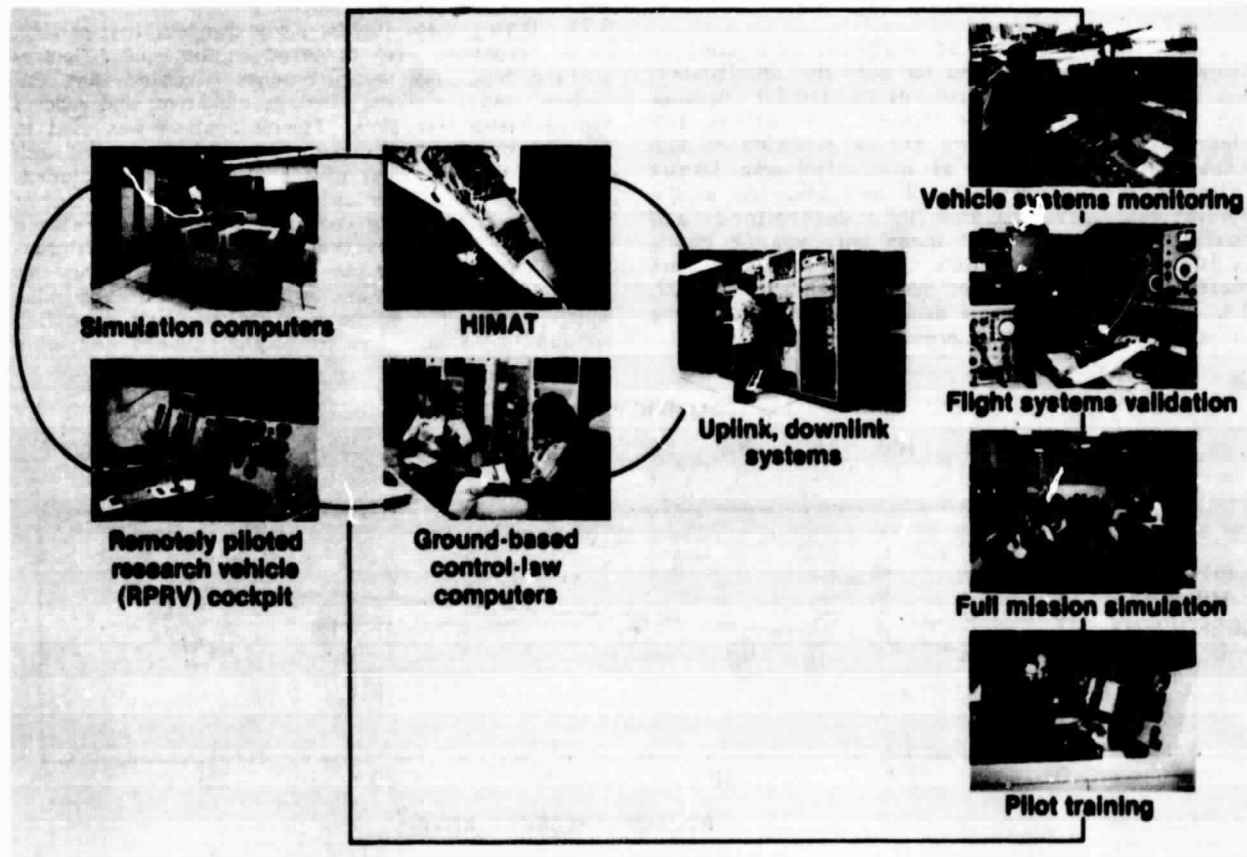

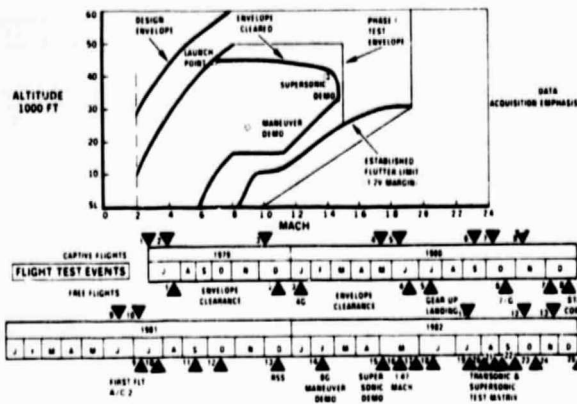
Figure 14. Iron Bird Simulation

7

Figure 15. HiMAT Flight Test Program Summary

vehicle landed with the landing gear retracted; it suffered only minor damage. It was not until the thirteenth flight that the number 2 vehicle flew with the relaxed static stability control laws. The maneuver and supersonic stability demonstration goals were achieved on the fourteenth and fifteenth flights respectively. The twelve flights in the final nine months of the program were very productive in gathering research results.

RESULTS

The HiMAT program produced many results. A few selected conclusions and comparisons conclude this paper.

A complete set of stability and control characteristics was obtained for both the longitudinal and lateral-directional degrees of freedom.[5] Because the actual values of the HiMAT derivatives are classified, the data shown are on unlabeled vertical axes. An assessment of predicted and flight determined derivatives can still be made. All of the derivatives, predicted and flight determined, are corrected to 0 percent mean aerodynamic chord (MAC). Figure 16 shows the pitching moment coefficient as a function of dynamic pressure at mach 0.8. From these and other derivatives, it appears that there were no significant aeroelastic effects.

Measured and predicted values of selected control derivatives as a function of angle of attack at mach 0.9 are shown in Figure 17. Because of the large differences between the wind tunnel-determined and flight-determined derivatives acquired with the vehicle statically stable, it was decided to reevaluate the lateral-directional control laws designed for the relaxed stability configuration. This led to a redesign of the lateral-directional control laws using the flight data base. These differences between flight and prediction also caused extensive simulator revision.
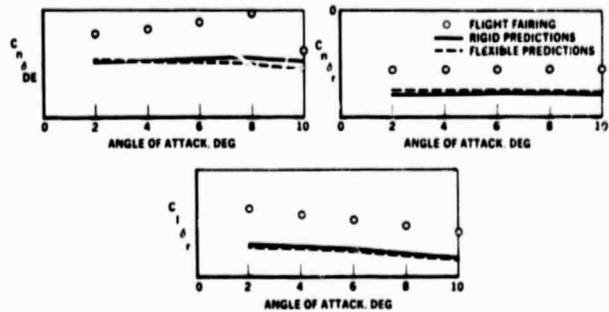

Figure 17. Comparison of Selected Control Derivatives as a Function of Angle of Attack at Mach 0.9

Trends in the damping measurements of the wing and canard flutter accelerometer data obtained in the transonic mach range at altitudes of 40,000 feet and 25,000 feet from the second and third flights indicated that there was insufficient damping in the canard, and that it could possibly flutter at approximately mach 0.95. During these flights, lowly damped, first-bending mode responses also occurred on the wing. Control surface free-play measurements revealed that the canard flaps, elevons, ailerons, elevators, and rudders had excessive free play. Flutter analysis was used to predict the flutter characteristics of the canard with the measured free play of the canard flaps included. The results of these calculations predicted flutter damping and frequency characteristics that correlated well with those observed in the previous flights. Subsequently, the free play on all control surfaces was reduced by tightening the control surface linkage bolts, which were found to be well below their specified torque. On the fourth flight, canard and wing
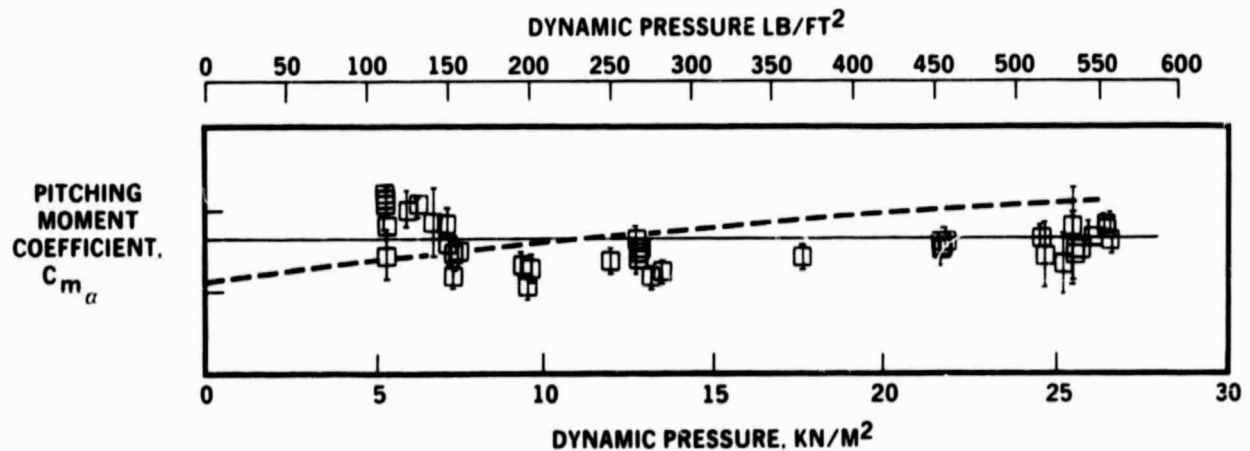

Figure 16. Aeroelastic Effects on Pitching Moment at Mach 0.8; Angle of Attack of 6.4 Degrees

8

damping showed stable trends to mach 0.925; the increases in damping were 300 to 400 percent over the results from the third flight (Figure 18). These trends indicated that classic transonic flutter would not be a problem.
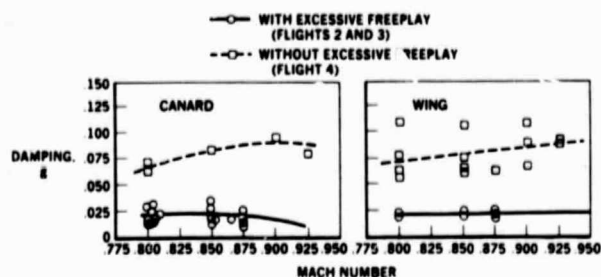

Figure 18. Comparison of Canard and Wing Modal Damping Characteristics With and Without Excessive Control Surface Free Play at 25,000 Feet

To accomplish the HiMAT research objectives, three maneuver types were required to be repeatedly flown with great precision. These maneuvers were pushover pullups, excess-thrust windup turns, and thrust-limited turns. The precision required for these maneuvers necessitated the development of a technique to provide automatic multiaxis control. A flight test maneuver autopilot (FTMAP) was developed to fly the HiMAT during these critical maneuvers.(6) Figure 19 compares two windup turns, nominally at the HiMAT design point of mach 0.9, 25,000 feet altitude, and 8g normal acceleration. The figure compares a pilot-flown and FTMAP-flown maneuver. While neither of

these turns completely achieves the precision required, the FTMAP-flown maneuver is more regular and controlled than the pilot-flown maneuver. The FTMAP does meet the precision requirements, except for a slight mach number decrease near the end of the maneuver. The FTMAP provided predictable and repeatable maneuvers from flight to flight and thus greatly improved the quality of the acquired flight test data.

Pressure-distribution measurements were made on the HiMAT air vehicle at seven locations on the wing, canard, and winglet.(6) These chordwise rows of pressure measurements were used to evaluate the performance of the lifting surfaces throughout the flight envelope, with special emphasis at the transonic-maneuver condition. The pressure distributions for the maneuver flight condition are presented in Figure 20 for two span stations located on the outboard wing panel. Here the wing is operating close to the design optimum. As can be seen, the agreement of the pressure coefficients between flights is very good. The leading-edge pressure peaks are reproduced faithfully between flights, as is the trailing edge recovery. The comparisons between the predicted and measured pressure distributions are classified, but, suffice it to say that while the agreement was reasonable, room for improvement certainly exists.

As previously discussed, it was determined during the aerodynamic design process that 9.5-degree twist (washout) at the wingtip was required to meet the sustained 8g maneuver goal. After thoroughly exercising the structural design process, it was concluded that an aeroelastic twist increment of 5.5 degrees was the maximum that could be expected. Thus, to achieve a 9.5-degree twist at the maneuver design point, it was necessary to build in a 4-degree twist in the jig (unloaded) shape for the wing.
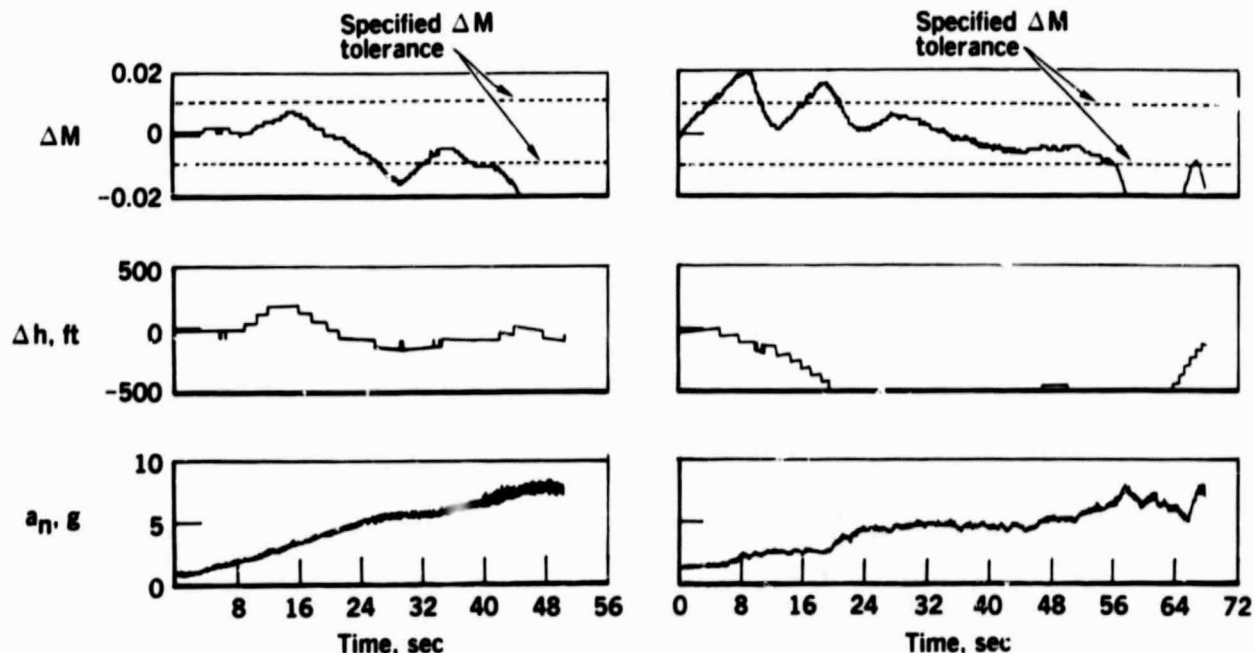

Figure 19. Comparison of Pilot and FTMAP-Flown Windup Turns at 8g, Mach 0.9, at 25,000 Feet
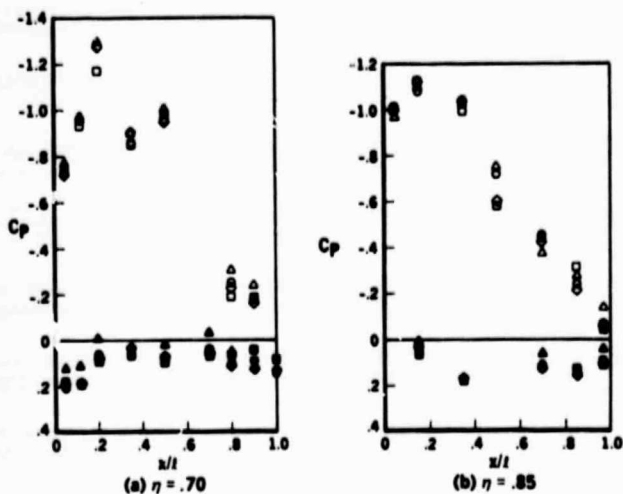
Figure 20. Wing Pressure Distribution for Maneuvering Flight at Mach 0.9, $\bar{q}$ = 440 lb/sq ft, α = 10°

A NASTRAN model of the HiMAT wing was developed and used to predict the twist at the wingtip at the maneuver design condition. The dashed line in Figure 21 shows the streamwise twist distribution of the wing using the NASTRAN model with predicted bending loads. This prediction indicated about 5-degree twist should be realized at the wingtip. Actual proof loading of the aircraft with wing attached after assembly resulted in a twist distribution shown by the solid line in Figure 21.(7) The flight measured loads were then extrapolated to the design maneuver condition using the proof load test results as reference with the solid symbols indicating actual twist distribution at mach 0.9, 25,000 feet, and 8g. Thus, it appears that the NASTRAN model of the HiMAT wing overpredicted the streamwise twist of the outer wing panel by 1.5 degrees.(8) This difference is apparently the result of modeling approximations employed to create the finite element model and lack of a material characterization data base for non-standard
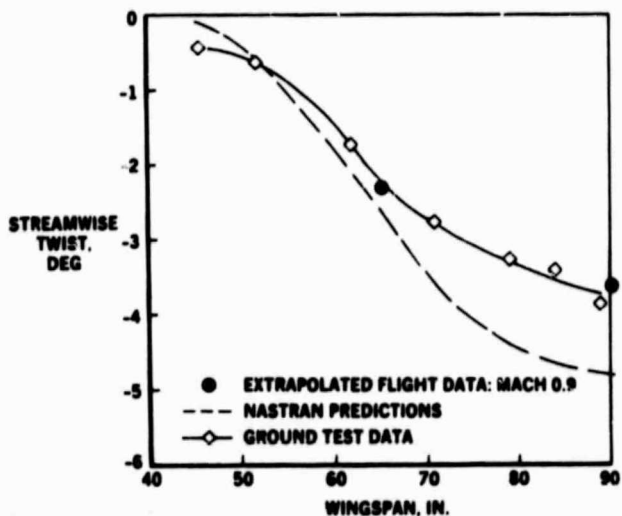
ply lay-up. It should be noted that even though the outer wing panel was flexible as indicated by the twist achieved, there were no significant effects of flexibility evident in the stability and control data.

Summary

The HiMAT program was highly successful in that the maneuver goals were demonstrated and flight evaluation of several highly interactive, high-risk technologies was achieved. The absence of a pilot in the cockpit did limit the ability to collect flying qualities and man-in-the loop data for assessment of the configuration. The HiMAT program also demonstrated the ability to design and fabricate a high performance airplane capable of meeting performance goals with a minimum of wind tunnel and ground testing. The HiMAT program (Figure 22) has provided the opportunity to close the design loop on an advanced fighter design by comparing flight test results with initial predictions and using the differences between them to refine and sharpen our design tools. The next design effort will be even better.
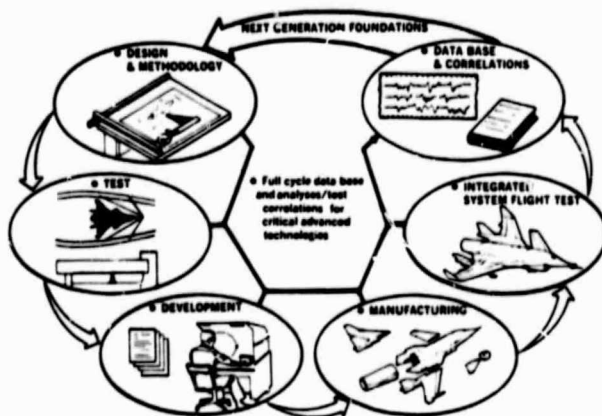
Figure 22. HiMAT Program Cycle

Figure 21. Comparison of Extrapolated Flight Test Results to Ground Test Data at the Maneuver Design Point

REFERENCES

1. Petersen, Kevin L., "Flight Control Systems Development of Highly Maneuverable Aircraft Technology (HiMAT) Vehicle," AIAA Paper 79-1789, Aug. 1979.

2. Gingrich, P. B., Child, R. D., and Panageas, G. N., "Aerodynamic Configuration Development of the Highly Maneuverable Aircraft Technology Remotely Piloted Research Vehicle," NASA CR-143841, 1977.

3. Price, M. A., "HiMAT Structural Development Design Methodology," NASA CR-144886, 1979.

4. Evans, Martha B., and Schilling, Lawrence J., "The Role of Simulation in the Development and Flight Test of the HiMAT Vehicle," NASA TM 84912, 1984.

5. Matheny, Neil W., and Panageas, George N., "HiMAT Aerodynamic Design and Flight Test Experience," AIAA Paper 81-2433, Nov. 1981. (AIAA Flight Test Conference, Las Vegas, Nevada)

6. Duke, E. L., and Lux, D. P., "The Application and Results of a New Flight Test Technique," AIAA Paper 83-2137, Aug. 1983.

7. Monaghan, Richard C., "Description of the HiMAT Tailored Composite Structure and Laboratory Measured Vehicle Shape Under Load," NASA TM 81354, 1981.

8. DeAngelis, V. M., "In-Flight Deflection Measurement of the HiMAT Aeroelastically Tailored Wing," AIAA Paper 81-24250, Nov. 1981.